Effect of repulsive and attractive interactions on depletion forces in colloidal suspensions: A density functional theory treatment

S. A. Egorov
Department of Chemistry, University of Virginia, Charlottesville, Virginia 22901, USA
(Received 2 May 2004; published 24 September 2004)

The author employs density functional theory to study colloidal interactions in solution. Hardcore Yukawa potentials with soft tails, either repulsive or attractive, are used to model colloid-solvent and solvent-solvent interactions. We analyze the effect of these interactions on the solvent-mediated potential of mean force between two colloids in solution. Overall, theory is shown to be in good agreement with recent simulation data. We use the theory to study the density dependence of the colloid-colloid second virial coefficient.

DOI: 10.1103/PhysRevE.70.031402 PACS number(s): 82.70.Dd, 61.20.Gy

I. INTRODUCTION

Numerous systems of biological and technological interest can be modeled as spherical colloidal particles dispersed in a solution of smaller colloidal particles (depletants) [1]. Understanding of the phase behavior and stability of such mixtures is of primary importance for the development of various industrial applications. A common method of constructing phase diagrams of colloidal dispersions involves adopting the McMillan-Mayer approach, whereby the real two-component mixture is modeled as a pseudo-one-component system, with colloidal particles interacting under the effective potential of mean force (PMF) induced by the depletant. The particular structure of the depletant-mediated PMF is quite sensitive to the character of colloid-depletant and depletant-depletant interactions [2]. In real systems, these interactions can be easily adjusted by varying such parameters as salt concentration or surface charge, which makes it possible to modify the effective PMF between the colloidal particles. Accordingly, it is important to develop accurate theoretical methods for calculating the effective PMFs that would be suitable for various forms of interparticle interaction potentials.

While the majority of previous theoretical studies of colloidal dispersions [3–9] have focused on the hard-sphere interactions (both additive and nonadditive), several workers [10–15] have analyzed the behavior of the colloid-colloid PMF when either attractive or repulsive soft interactions are added to hard-core repulsions. A particularly extensive study was performed by Louis *et al.* [16] who employed a microscopic model based on hardcore Yukawa potentials, which allowed them to consider various combinations of repulsive and attractive colloid-depletant and depletant-depletant soft interactions. These authors have performed molecular dynamics (MD) simulations to obtain exact results for the PMF for each of the systems studied. The following general trends were observed. Adding a colloid-depletant soft repulsion enhanced the depletion attraction between the two colloids (which was further enhanced by the addition of depletant-depletant soft attraction), since both these interactions reduce the depletant density in the vicinity of the colloids. Conversely, adding a colloid-depletant soft attraction results in the accumulation of the depletant around the colloids, which makes the effective colloid-colloid PMF more repulsive. While the addition of a soft repulsion between depletants enhances the accumulation repulsion between colloids, the same effect can be achieved by adding a depletant-depletant *attraction*, in which case the two attractive interactions (colloid-depletant and depletant-depletant) produce a mutually amplified enhancement of the depletant density around the colloids [16].

While computer simulations provide a valuable tool for obtaining exact results for the structural properties of colloidal dispersions, these calculations are rather time consuming. For the purpose of exploring the large parameter space covered by the model interaction potential parameters, it would be more practical to employ a theoretical method to compute the PMF. Louis *et al.* [16] have assessed the accuracy of two such methods by comparing theoretical results with computer simulation data. The first method is based on the Kirkwood superposition approximation (KSA) [6,17], where the anisotropic depletant density profile induced by two colloids is approximated by the product of isotropic density profiles around individual colloids (the latter were taken directly from computer simulations). It was found that the KSA approach yielded accurate results in the case of repulsive colloid-depletant soft interactions (when the local density around colloids was depleted), but broke down for attractive interactions (when local density was enhanced). Furthermore, it is well established [6], that the quality of KSA decreases with increasing solvent packing fraction. The other theoretical method tested by Louis *et al.* is based on the density functional theory (DFT). They considered a particular implementation of DFT, where the hardcore Yukawa mixture with repulsive/attractive soft interactions was mapped onto an effective hard-sphere mixture, for which highly accurate DFT methods are available [8]. It was found that the mapping onto nonadditive mixtures performed well for repulsive depletant-depletant interaction, but underestimated the effective PMF for the attractive case. The performance of the mapping procedure was especially poor when both colloid-depletant and depletant-depletant interactions were attractive, since the hard-sphere mapping could not capture the nonlinear mutual enhancement of the depletant density leading to "repulsion through attraction" [16]. Thus, neither of the theoretical methods tested was in quantitative agree-

ment with simulation for all systems studied, which highlights the necessity for developing alternative theoretical approaches to treat colloidal mixtures with soft interactions.

Quite recently, a novel method was proposed to study structural properties of systems where both hardcore repulsions and soft tail attractions are present [18]. The method is formulated within the DFT framework based on the weighted density approximation (WDA). The excess free energy functional is split into two terms corresponding to repulsive and attractive interactions. In addition, two separate weighting functions and weighted densities are introduced for repulsive and attractive terms. The method was applied to study polymer density profiles at surfaces and was found to be in good agreement with simulations. We note that such approach would be ideally suited for systems based on the Yukawa model potentials, which naturally split into a hardcore repulsive wall and a soft tail (either repulsive or attractive). Furthermore, a closed analytical form was recently obtained for the Yukawa excess free energy functional [19], which was shown to be highly accurate for both repulsive and attractive Yukawa tails [11,19]. In the present work, we employ the DFT method of Müller *et al.* [18] to study colloidal interactions in hardcore Yukawa mixtures. We show that theory is in quantitative agreement with simulations for all systems studied by Louis *et al.* [16], except for the one involving both colloid-depletant and depletant-depletant attractions. We also perform model theoretical calculations for a wide range of depletant packing fractions (not studied in the simulations) and compute the density dependence of the colloid-colloid second virial coefficient.

The remainder of the paper is organized as follows. In Sec. II we specify our microscopic model and outline the DFT approach employed to compute the interaction between two dilute colloidal particles in solution. In Sec. III we compare our theoretical results with computer simulations and perform model studies of effective interactions between colloidal particles. In Sec. IV we conclude.

II. MICROSCOPIC MODEL AND DENSITY FUNCTIONAL THEORY

We consider two spherical colloidal particles present at infinite dilution in a solvent composed of spherical molecules. The diameters of colloidal and solvent (depletant) particles are denoted by σ_{cc} and σ_{ss}, respectively. The solvent particles interact via isotropic pairwise potential of the hard-sphere Yukawa form,

$$\phi_{ss}(r) = \begin{cases} \epsilon_{ss}\sigma_{ss}\,\exp[-\kappa_{ss}(r-\sigma_{ss})]/r, & r \geqslant \sigma_{ss}, \\ \infty, & r < \sigma_{ss}. \end{cases} \tag{1}$$

The colloid-solvent potential has the same functional form, but with different parameters,

$$\phi_{cs}(r) = \begin{cases} \epsilon_{cs}\sigma_{cs}\,\exp[-\kappa_{cs}(r-\sigma_{cs})]/r, & r \geqslant \sigma_{cs}, \\ \infty, & r < \sigma_{cs}, \end{cases} \tag{2}$$

where $\sigma_{cs}=(\sigma_{cc}+\sigma_{ss})/2$.

For the bare interaction potential between the two colloidal particles we take the hard-sphere form

$$\phi_{cc}(r) = \begin{cases} 0, & r \geqslant \sigma_{cc}, \\ \infty, & r < \sigma_{cc}. \end{cases} \tag{3}$$

The total potential of mean force (PMF) between two colloidal particles in solution can be written as the sum of the bare potential and the solvent-mediated PMF,

$$\Phi_{cc}(r) = \phi_{cc}(r) + W(r). \tag{4}$$

The calculation of the solvent-mediated PMF $W(r)$ is the main goal of the present study.

In order to obtain $W(r)$, we define $\rho(\vec{r},R)$ as the conditional probability of finding a solvent particle at $\vec{r}$ given that one colloid is at the origin and the other is located at $\vec{R}$. With this definition, the solvent mediated PMF between the two colloids is given by the following exact relations [17]:

$$W(R) = \int_R^\infty F(R')dR', \tag{5}$$

where the excess mean force, $F(R)$, is given by

$$F(R) = -\int d\vec{r}[\nabla\phi_{cs}(r)\cdot\hat{\mathbf{R}}]\rho(\vec{r};R), \tag{6}$$

where $\hat{\mathbf{R}}$ is the unit vector along $\vec{\mathbf{R}}$.

It is clear from the above that $\mathbf{R}$ is completely determined by the anisotropic solvent density profile induced by the two colloids. By treating the two colloidal particles as a source of an external field, we can employ the standard DFT formalism to obtain the equilibrium density profile of the fluid in an external potential. The starting point of the DFT treatment is the expression of the grand free energy, Ω, as a functional of the solvent density profile. The minimization of Ω with respect to $\rho(\vec{r},R)$ yields the equilibrium solvent density distribution.

The functional Ω is related to the intrinsic Helmholtz free energy functional, F, via a Legendre transform,

$$\Omega[\rho(\vec{r},R)] = F[\rho(\vec{r},R)] + \int d\vec{r}\,\rho(\vec{r},R)[\phi_{\text{ext}}(\vec{r},R)-\mu], \tag{7}$$

where μ is the chemical potential and $\phi_{\text{ext}}(\vec{r},R)$ is the external field, which in the present case is due to the interaction of the solvent with colloids $\phi_{\text{ext}}(\vec{r},R)=\phi_{cs}(r)+\phi_{cs}(|\vec{r}-\vec{R}|)$.

The intrinsic Helmholtz free energy functional can be separated into ideal and excess parts,

$$F[\rho(\vec{r},R)] = F_{\text{id}}[\rho(\vec{r},R)] + F_{\text{ex}}[\rho(\vec{r},R)], \tag{8}$$

with the ideal functional known exactly,

$$F_{\text{id}}[\rho(\vec{r},R)] = \beta^{-1}\int d\vec{r}\,\rho(\vec{r},R)\{\ln[\Lambda^3\rho(\vec{r},R)]-1\}, \tag{9}$$

where Λ is the thermal de Broglie wavelength and $\beta^{-1}=k_BT$.

Following the earlier DFT study of systems with repulsive and attractive interactions [18], we decompose the excess free energy functional into contributions arising from harsh

hard-sphere repulsions and soft Yukawa tail interactions [the latter can be either repulsive or attractive depending on the sign of ϵ_{ss} in Eq. (1)]:

$$F_{\mathrm{ex}}[\rho(\vec{r},R)] = F_{\mathrm{hs}}[\rho(\vec{r},R)] + F_{\mathrm{tail}}[\rho(\vec{r},R)]. \tag{10}$$

In the present study we obtain both F_{hs} and F_{tail} within the weighted density approximation [20],

$$F_{\mathrm{hs}}[\rho(\vec{r},R)] = \int d\vec{r}\, \rho(\vec{r},R) f_{\mathrm{hs}}(\overline{\rho}_{\mathrm{hs}}(\vec{r},R)), \tag{11}$$

and

$$F_{\mathrm{tail}}[\rho(\vec{r},R)] = \int d\vec{r}\, \rho(\vec{r},R) f_{\mathrm{tail}}(\overline{\rho}_{\mathrm{tail}}(\vec{r},R)), \tag{12}$$

where $f_{\mathrm{hs}}(\rho)$ and $f_{\mathrm{tail}}(\rho)$ are the excess free energies per particle (evaluated at the fluid density ρ) arising from the hard-sphere repulsions and soft tail interactions, respectively. The weighted densities $\overline{\rho}_{\mathrm{hs}}(\vec{r},R)$ and $\overline{\rho}_{\mathrm{tail}}(\vec{r},R)$ are defined according to

$$\overline{\rho}_{\mathrm{hs}}(\vec{r},R) = \int d\vec{r}'\, \rho(\vec{r}',R) w_{\mathrm{hs}}(|\vec{r}-\vec{r}'|) \tag{13}$$

and

$$\overline{\rho}_{\mathrm{tail}}(\vec{r},R) = \int d\vec{r}'\, \rho(\vec{r}',R) w_{\mathrm{tail}}(|\vec{r}-\vec{r}'|), \tag{14}$$

with the weighting functions satisfying the normalization condition

$$\int d\vec{r}\, w_{\mathrm{hs}}(r) = \int d\vec{r}\, w_{\mathrm{tail}}(r) = 1. \tag{15}$$

We note that the form of the hard-sphere component of the excess free energy functional, as given by Eq. (11), is due to Tarazona [20]. While more accurate functionals are currently available, such as the one based on the Rosenfeld's fundamental measure theory (FMT) [21], for the sake of simplicity we have restricted ourselves to the Tarazona form. A comparison of our theoretical results with simulation and with FMT-based DFT calculations of Roth *et al.* [9] appears to indicate that the Tarazona functional is adequate for our purposes.

The minimization of the grand free energy yields the following result for the equilibrium solvent density profile:

$$\begin{aligned}\rho(\vec{r};R) = \rho_b \exp\Big[& -\beta\{\phi_{cs}(r) + \phi_{cs}(|\vec{r}-\vec{R}|) + f_{\mathrm{hs}}(\overline{\rho}_{\mathrm{hs}}(\vec{r},R)) \\ & + \int d\vec{r}'\, \rho(\vec{r}',R) w_{\mathrm{hs}}(|\vec{r}-\vec{r}'|) f'_{\mathrm{hs}}(\overline{\rho}_{\mathrm{hs}}(\vec{r},R)) \\ & + f_{\mathrm{tail}}(\overline{\rho}_{\mathrm{tail}}(\vec{r},R)) + \int d\vec{r}'\, \rho(\vec{r}',R) w_{\mathrm{tail}}(|\vec{r}-\vec{r}'|) \\ & \times f'_{\mathrm{tail}}(\overline{\rho}_{\mathrm{tail}}(\vec{r},R)) - f_{\mathrm{hs}}(\rho_b) - \rho_b f'_{\mathrm{hs}}(\rho_b) - f_{\mathrm{tail}}(\rho_b) \\ & - \rho_b f'_{\mathrm{tail}}(\rho_b)\}\Big],\end{aligned} \tag{16}$$

where ρ_b is the bulk solvent density and $f' = df/d\rho$.

In order to compute $\rho(\vec{r};R)$ from Eq. (16), it remains to specify the free energy components $f_{\mathrm{hs}}(\rho)$ and $f_{\mathrm{tail}}(\rho)$, and the weighting functions $w_{\mathrm{hs}}(r)$ and $w_{\mathrm{tail}}(r)$. For the hard-sphere part of the free energy, we use the Carnahan-Starling equation of state,

$$\beta f_{\mathrm{hs}}(\rho) = \frac{4\eta - 3\eta^2}{(1-\eta)^2}, \tag{17}$$

where $\eta = \pi\rho\sigma_{ss}^3/6$ is the solvent packing fraction. For the contribution to the free energy arising from the Yukawa tail, we use an approximate analytic expression derived by Duh *et al.* [19], which was shown to provide very accurate free energy results both for repulsive and attractive hard-sphere Yukawa fluids [11,19]. The expression for f_{tail} obtained by Duh *et al.* [19] is reproduced in the Appendix.

Regarding the choice of the weighting functions, we follow the earlier density functional study, where the range of $w_{\mathrm{hs}}(r)$ was taken to be the solvent hard-sphere diameter, while the range of $w_{\mathrm{tail}}(r)$ was identified with the range of the tail of $\phi_{ss}(r)$. Accordingly, we take the simple form for $w_{\mathrm{hs}}(r)$,

$$w_{\mathrm{hs}}(r) = \frac{3}{4\pi\sigma_{ss}^3}\Theta(\sigma_{ss} - r), \tag{18}$$

where $\Theta(r)$ is the Heaviside step function. For $w_{\mathrm{tail}}(r)$ we employ the following form:

$$w_{\mathrm{tail}}(r) = \frac{\phi_{\mathrm{tail}}(r)}{4\pi\int_0^\infty dr\, r^2 \phi_{\mathrm{tail}}(r)}, \tag{19}$$

where

$$\phi_{\mathrm{tail}}(r) = \begin{cases} \phi_{ss}(r), & r \geqslant \sigma_{ss}, \\ \phi_{ss}(\sigma_{ss}), & r < \sigma_{ss}. \end{cases} \tag{20}$$

With the above choices for free energy components and weighting functions, we solve Eq. (16) iteratively. Taking advantage of the cylindrical symmetry of the problem, the anisotropic solvent density profile is constructed on a two-dimensional (r,θ) grid, and the convolution integrals in Eq. (16) are performed by expanding the corresponding functions in Legendre polynomials. We found that using 200 polynomials was sufficient to obtain converged results. The step size along the radial coordinate of the grid was taken to be $0.05\sigma_{ss}$, and the total number of points along this coordinate was taken to be 500. We note that the central point of our grid ($r=0$) is located at the center of one of the colloidal particles. Accordingly, the grid points with $r=\sigma_{cs}$ yield the contact values of the solvent density. This is important, because in the absence of the Yukawa tail in the colloid-solvent interaction potential, the depletion force [given by Eq. (6)] is entirely determined by the contact density.

Once the anisotropic solvent density profile was calculated, the excess mean force between two colloidal particles was obtained from Eq. (6), and the solvent mediated PMF was computed from Eq. (5). In the next section, we compare our DFT results with previously published computer simulations, and present results of our model calculations.

TABLE I. Parameter combinations for interaction potentials.

System	$\beta\epsilon_{bs}$	$\beta\epsilon_{ss}$
1	0	0
2	0	2.99
3	0	−0.996
4	0.82	0
5	0.82	2.99
6	0.82	−0.996
7	−0.82	0
8	−0.82	2.99
9	−0.82	−0.996

III. COMPARISON OF THEORY WITH SIMULATION AND MODEL CALCULATIONS

In order to test the accuracy of the DFT treatment presented in the preceding section, we compare our theoretical results with recently published computer simulation data of Louis *et al.* [16] These authors have performed MD simulations of effective forces between two dilute spherical colloidal particles in a spherical solvent, with interaction potentials given by Eqs. (1)–(3). The potential parameters used in the simulations are listed in Table I. Three choices for both colloid-solvent and solvent-solvent interactions were considered: pure hard-sphere repulsion, a hard-sphere repulsion combined with a repulsive Yukawa tail, and a hard-sphere repulsion combined with an attractive Yukawa tail. All possible combinations of these choices yield nine systems listed in Table I. The values of remaining parameters were fixed as follows: $\sigma_{cc}=5\sigma_{ss}$, $\kappa_{ss}=3/\sigma_{ss}$, and $\kappa_{cs}=1.2/\sigma_{cs}$. The solvent packing fraction in all the simulations was set to be $\eta_b^* = \pi\rho_b\sigma_{ss}^3/6=0.1$.

We start by calculating the (spherically symmetric) solvent density profile around a *single* colloidal particle for each of the nine model systems. Our theoretical results together with the simulation data [16] are shown in Figs. 1–3. One sees that the solvent density profiles yielded by the DFT are in good agreement with the simulation for all nine systems studied. In particular, DFT successfully reproduces all the trends predicted by the simulation regarding the effects of the colloid-solvent and solvent-solvent soft repulsive and attractive interactions on the accumulation of the solvent particles near the colloidal sphere. Namely, for a given colloid-solvent interaction, a soft repulsive solvent-solvent interaction (in addition to the hard-sphere repulsion) results in an additional accumulation of the solvent near the colloid, while solvent-solvent attraction produces an opposite effect. The only exception is observed for system 9, where both colloid-solvent and solvent-solvent interactions contain an attractive tail. In the latter case, the contact value of the solvent density profile at the colloidal surface is still smaller compared to the hard-sphere solvent (in agreement with the trend discussed above), but there is a pronounced accumulation of the solvent in the *second* solvation shell. As discussed by Louis *et al.* [16], this effect is due to the mutual nonlinear amplification of colloid-solvent and solvent-solvent attractive interactions, which makes it favorable for the solvent to cluster near the colloid.

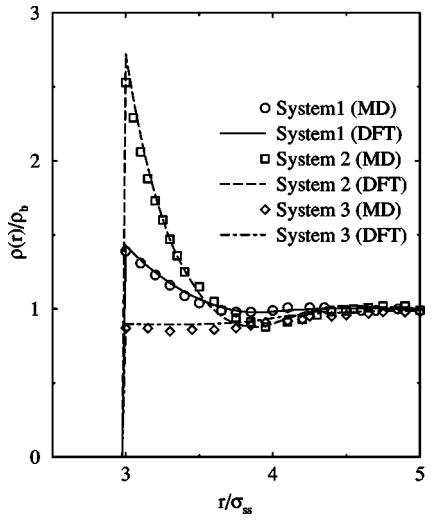

FIG. 1. Normalized density profiles of solvent particles around a single colloidal sphere for systems 1–3, with model potential parameters listed in Table I. Symbols are from the published simulation data of Louis *et al.* [16], and lines are from the DFT method.

We now turn to the discussion of excess mean force and solvent mediated PMF between two colloidal particles in solution. The simulation [16] and theoretical results for the forces are shown in Figs. 4–6, while the PMF results are presented in Figs. 7–9. Once again, DFT is in good agreement with simulation, with the only significant discrepancy observed for system 9, where theory does not capture the long range nature of the repulsive force between two colloids, and, as a result, somewhat underestimates the magnitude of the corresponding repulsive PMF (lower panels of Figs. 6 and 9, respectively). The general trends predicted by the simulation and successfully reproduced by the theory are as follows. For a given solvent-solvent interaction, the addition of the soft repulsive tail to the colloid-solvent interaction enhances attraction between the two colloids, while an at-

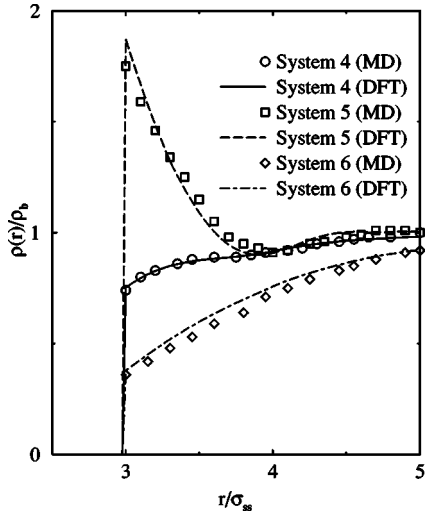

FIG. 2. Same as Fig. 1, but for systems 4–6.

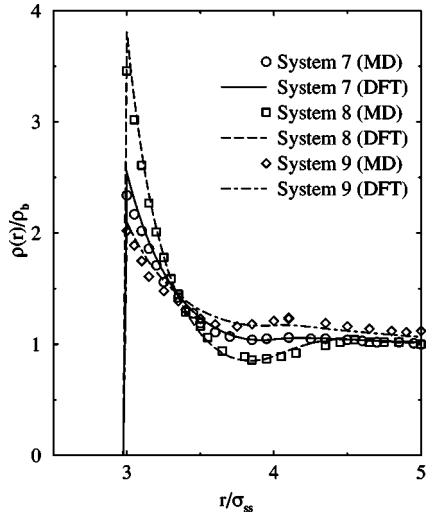

FIG. 3. Same as Fig. 1, but for systems 7–9.

tractive colloid-solvent interaction increases colloid-colloid repulsion. The former effect is due to the standard "attraction due to depletion" mechanism, since a repulsive colloid-solvent potential results in depleted solvent density around the colloids (see Figs. 1–3), which enhances the attraction between them. By contrast, the accumulation of the solvent around "attractive" colloids leads to steric repulsion. The same effect can be achieved for a given colloid-solvent interaction by adding a soft repulsive component to the solvent-solvent interaction, which again leads to the solvent accumulation near the colloidal surface and the concomitant steric repulsion between the colloids. In the latter case, the solvent mediated PMF develops an oscillatory structure (clearly seen in the middle panel of Fig. 7), which would become even more pronounced at higher solvent densities. By the same argument, one would expect that an additional

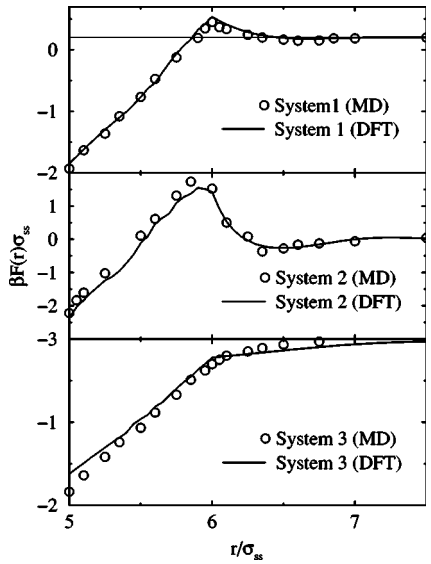

FIG. 4. The dimensionless excess mean force between two colloidal particles for systems 1–3. Symbols are from the published simulation data of Louis *et al.* [16], and lines are from the DFT method.

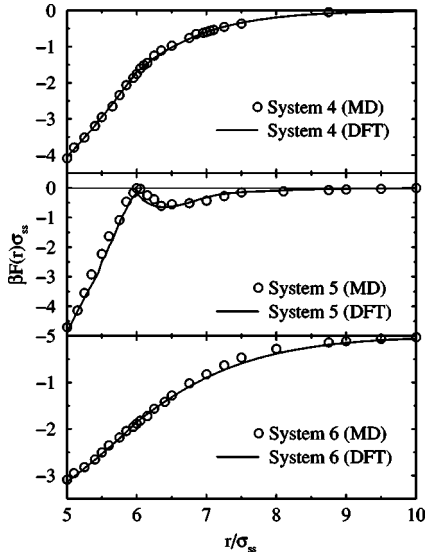

FIG. 5. Same as Fig. 4, but for systems 4–6.

solvent-solvent attraction, which generally depletes the solvent density at the colloidal surface, would induce a depletion attraction between the colloids. This is indeed observed for the cases of hard sphere and "hard sphere plus soft repulsion" colloid-solvent interaction potentials. The exception to this rule is provided by system 9, where colloid-solvent interaction is attractive. As already discussed above, the nonlinear mutual amplification of colloid-solvent and solvent-solvent attractions produces solvent accumulation in the second solvation shell around the colloids, which, in turn, leads to an additional steric repulsion seen in the simulated PMF (lower panel of Fig. 9). Theory does not quite capture this subtle effect, since it misses the long-range repulsive tail in the excess mean force (lower panel of Fig. 6).

Having ascertained the accuracy of the proposed DFT treatment, we now use it to perform model calculations of colloidal interactions at higher solvent densities (not studied

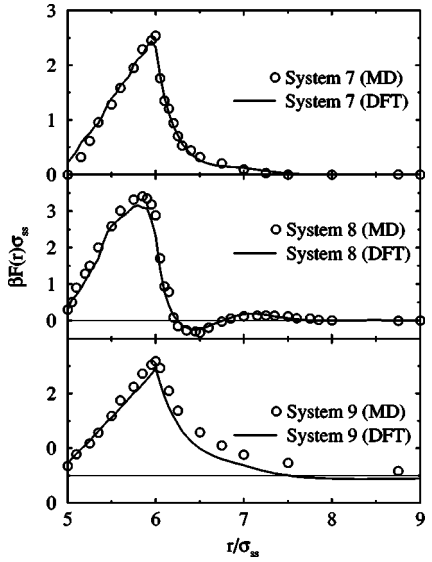

FIG. 6. Same as Fig. 4, but for systems 7–9.

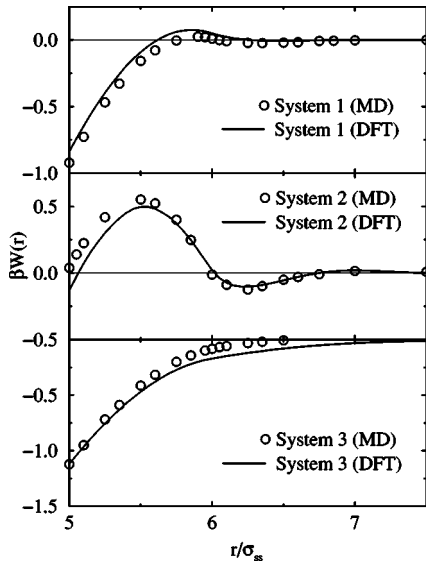

FIG. 7. The potential of mean force between two colloidal particles for systems 1–3. Symbols are from the published simulation data of Louis *et al.* [16], and lines are from the DFT method.

in the simulations). We have considered (dimensionless) solvent packing fractions η_b^* spanning the range between 0 and 0.3. Our theoretical calculations have shown that for systems 3, 4, 5, and 6, where the PMF is purely attractive at $\eta_b^* = 0.1$, it becomes progressively more attractive as the solvent density is increased. For the remaining systems, where the PMF exhibits a repulsive barrier at close colloidal separations, the height of this barrier increases with η_b, and pronounced oscillations develop at larger separations.

In order to present our results in a compact way, we now discuss the density behavior of the colloid-colloid second virial coefficient, which can be computed from the PMF as follows:

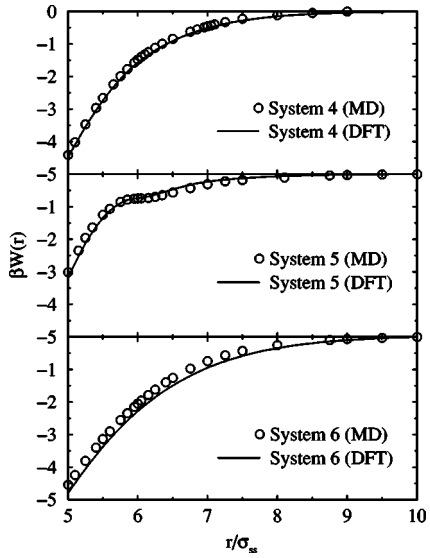

FIG. 8. Same as Fig. 7, but for systems 4–6.

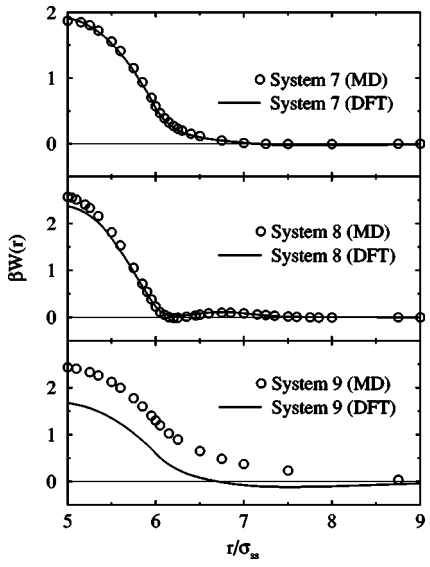

FIG. 9. Same as Fig. 7, but for systems 7–9.

$$B_2 = 2\pi \int_{\sigma_{cc}}^{\infty} dr\, r^2 \{1 - \exp[-\beta \Phi_{cc}(r)]\}$$

$$= \frac{2}{3}\pi\sigma_{cc}^3 + 2\pi \int_{\sigma_{cc}}^{\infty} dr\, r^2 \{1 - \exp[-\beta W(r)]\}, \quad (21)$$

where the first term in the sum is the hard-sphere contribution and the second term gives the solvent-mediated contribution to B_2. The upper panel of Fig. 10 shows B_2 as a

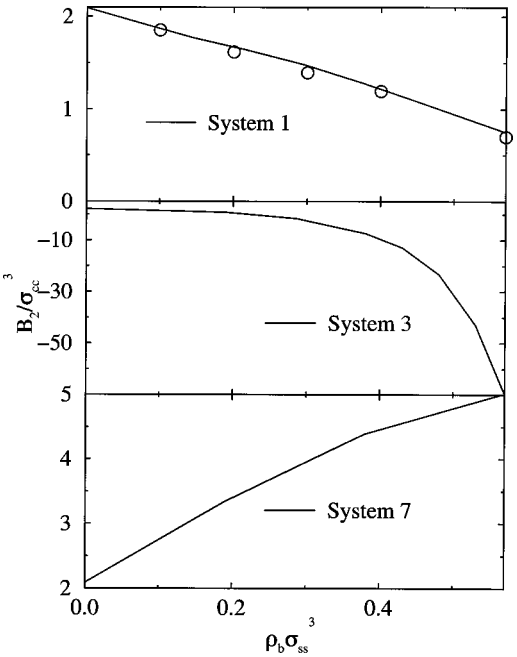

FIG. 10. The colloid-colloid second virial coefficient as a function of dimensionless solvent density. Upper panel, system 1, symbols are from the theory of Roth *et al.* [9], and lines are from the present DFT method. Middle panel, present DFT results for system 3. Lower panel, present DFT results for system 7.

function of dimensionless solvent density for system 1, where all interparticle interactions are hard-sphere repulsions. Our theoretical results are plotted as a solid line, while symbols denote the results of highly accurate theoretical method due to Roth *et al.* [9], which is based on the potential distribution theorem [8]. One sees that both theoretical approaches are in good agreement with each other. The second virial coefficient decreases monotonically with ρ_b, indicating that the effective colloidal interaction becomes more attractive overall at higher densities (despite the increasing repulsive barrier at short separations). Similar behavior of B_2 is observed for system 2 (not shown), although the slope of $B_2(\rho_b)$ is somewhat smaller, which reflects an additional colloid-colloid repulsion arising from soft solvent-solvent repulsions in system 2.

The middle panel of Fig. 10 shows $B_2(\rho_b)$ for system 3, where soft solvent-solvent attraction is added to hard-sphere interactions. As discussed earlier, this enhances the depletion attraction between colloids. This effect becomes more pronounced with increasing solvent density. Indeed, B_2 is seen to be a rapidly decreasing function of ρ_b. Even steeper decrease of the virial coefficient with density is observed for the systems containing a soft colloid-solvent repulsion (systems 4–6), essentially irrespective of the nature of the solvent-solvent interactions.

Finally, systems 7–9 contain a soft colloid-solvent attraction, which produces an accumulation repulsion between the colloids. Again, this effect becomes stronger at higher solvent densities, as can be seen from the lower panel of Fig. 10, which depicts $B_2(\rho_b)$ for system 7. The second virial coefficient increases monotonically with the solvent density, indicating that the effective colloidal interaction becomes progressively more repulsive.

IV. CONCLUSION

In this work we have presented a theoretical study of colloidal interactions in solution. We have employed a microscopic model based on hardcore Yukawa potentials, which are composed of a hardcore repulsive wall and a soft tail. The latter can be either repulsive or attractive, which makes it possible to tune the soft component of colloid-solvent and solvent-solvent interactions from repulsive to attractive, thereby tailoring the effective colloid-colloid interactions. In order to compute the PMF between the two colloids, we used the DFT method recently proposed by Müller *et al.* [18], where the excess free energy functional is split into repulsive and attractive terms, and separate weighting functions and weighted densities are introduced for the two contributions. We compared our theoretical results for the solvent density profiles, the excess mean force, and the PMF with the MD simulation data of Louis *et al.* [16]. The theory was shown to be in quantitative agreement with the simulation, except for the case when both solvent-solvent and colloid-solvent interactions contain a soft attractive component.

The major advantage of theoretical methods over computer simulations is the possibility of exploring large parameter space much more rapidly. For example, while MD simulations were performed for a single fixed value of the solvent packing fraction, the DFT method allowed us to compute the colloid-colloid second virial coefficient as a function of the solvent density. We found that in the systems containing a soft colloid-solvent repulsive tail the second virial coefficient decreases very steeply with density, indicating a rapidly growing colloid-colloid depletion attraction. Conversely, in the presence of a soft colloid-solvent attraction, the second virial coefficient grows with density (albeit much less rapidly), indicating a gradually increasing repulsion through accumulation.

Finally, we note that the methods presented here can be easily extended to treat more complicated depletants, such as fully flexible hardcore Yukawa chains. Such polymeric depletants can display a more rich and varied behavior in comparison to simple spherical solvents. This will be the subject of our future research.

ACKNOWLEDGMENT

The author acknowledges financial support from the National Science Foundation through Grant No. CHE-0235768.

APPENDIX

Duh *et al.* [19] have recently derived an approximate analytic expression for the free energy of a hard-sphere Yukawa fluid, which is written as a sum of two terms: the hard-sphere part [given by Eq. (11)] and the contribution from the Yukawa tail. The latter is given by [19]

$$\beta f_{\text{tail}} = \frac{\alpha_0}{\Phi_0}\beta\epsilon_{ss} - \frac{z^3}{6\eta}\left[F(x) - F(y) - (x-y)\frac{dF(y)}{dy}\right], \tag{A1}$$

where $z = \kappa_{ss}\sigma_{ss}$ and

$$x = -\frac{(1+z\psi)w\beta\epsilon_{ss}}{z^2}, \tag{A2}$$

$$y = -\frac{w\psi\beta\epsilon_{ss}}{z}, \tag{A3}$$

$$F(x) = -\frac{1}{4}\ln(1-2x) - 2\ln(1-x) - \frac{3}{2}x - \frac{1}{1-x} + 1, \tag{A4}$$

$$\alpha_0 = \frac{L(z)}{z^2(1-\eta)^2}, \tag{A5}$$

$$\Phi_0 = \frac{e^{-z}L(z) + S(z)}{z^3(1-\eta)^2}, \tag{A6}$$

$$\psi = z^2(1-\eta)^2\frac{1-e^{-z}}{e^{-z}L(z)+S(z)} - 12\eta(1-\eta)\frac{1-z/2-(1+z/2)e^{-z}}{e^{-z}L(z)+S(z)}, \tag{A7}$$

$$w = \frac{6\eta}{\Phi_0^2}, \tag{A8}$$

with

$$L(z) = 12\eta[(1 + \eta/2)z + 1 + 2\eta], \tag{A9}$$

$$S(z) = (1 - \eta)^2 z^3 + 6\eta(1 - \eta)z^2 + 18\eta^2 z - 12\eta(1 + 2\eta). \tag{A10}$$

Free energy given by Eq. (12) was compared with simulation results for an extensive set of thermodynamic conditions, and was shown to be accurate for both repulsive and attractive hard-sphere Yukawa fluids [11,19].

[1] W. B. Russel, D. A. Saville, and W. R. Schowalter, *Colloidal Dispersions* (Cambridge University Press, Cambridge, 1989).
[2] L. Belloni, J. Phys.: Condens. Matter **12**, R549 (2000).
[3] S. Asakura and F. Oosawa, J. Chem. Phys. **22**, 1255 (1954).
[4] S. Asakura and F. Oosawa, J. Polym. Sci. **33**, 183 (1958).
[5] T. Biben and J. P. Hansen, Phys. Rev. Lett. **66**, 2215 (1991).
[6] T. Biben, P. Bladon, and D. Frenkel, J. Phys.: Condens. Matter **8**, 10799 (1996).
[7] R. Dickman, P. Attard, and V. Simonian, J. Chem. Phys. **107**, 205 (1997).
[8] R. Roth, R. Evans, and S. Dietrich, Phys. Rev. E **62**, 5360 (2000).
[9] R. Roth, R. Evans, and A. A. Louis, Phys. Rev. E **64**, 051202 (2001).
[10] S. Amokrane, J. Chem. Phys. **108**, 7459 (1998).
[11] H. H. von Grünberg and R. Klein, J. Chem. Phys. **110**, 5421 (1999).
[12] J. M. Mendez-Alcaraz and R. Klein, Phys. Rev. E **61**, 4095 (2000).
[13] S. A. Egorov and E. Rabani, J. Chem. Phys. **115**, 617 (2001).
[14] E. Rabani and S. A. Egorov, J. Chem. Phys. **115**, 3437 (2001).
[15] E. Rabani and S. A. Egorov, Nano Lett. **2**, 69 (2002).
[16] A. A. Louis, E. Allahyarov, H. Löwen, and R. Roth, Phys. Rev. E **65**, 061407 (2002).
[17] P. Attard, J. Chem. Phys. **91**, 3083 (1989).
[18] M. Müller, L. G. MacDowell, and A. Yethiraj, J. Chem. Phys. **118**, 2929 (2003).
[19] D. M. Duh and L. Mier-Y-Teran, Mol. Phys. **90**, 373 (1997).
[20] P. Tarazona, Mol. Phys. **52**, 81 (1984).
[21] Y. Rosenfeld, Phys. Rev. Lett. **63**, 980 (1989).